Article

Growth of *p*- and *n*-Dopable Films from Electrochemically Generated C$_{60}^{\cdot}$ Cations

Carlo Bruno, Massimo Marcaccio, Demis Paolucci, Carla Castellarin-Cudia, Andrea Goldoni, Alexey V. Streletskii, Thomas Drewello, Simona Barison, Alessandro Venturini, Francesco Zerbetto, and Francesco Paolucci

J. Am. Chem. Soc., **2008**, 130 (12), 3788-3796 • DOI: 10.1021/ja0733179

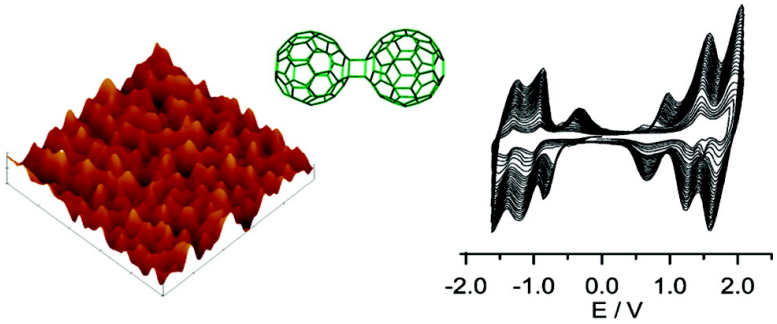

More About This Article

Additional resources and features associated with this article are available within the HTML version:

- Supporting Information
- Links to the 2 articles that cite this article, as of the time of this article download
- Access to high resolution figures
- Links to articles and content related to this article
- Copyright permission to reproduce figures and/or text from this article

View the Full Text HTML

J|A|C|S
ARTICLES
Published on Web 03/04/2008

Growth of *p*- and *n*-Dopable Films from Electrochemically Generated C_{60} Cations

Carlo Bruno,[†] Massimo Marcaccio,*[,†] Demis Paolucci,[†] Carla Castellarin-Cudia,[‡] Andrea Goldoni,[‡] Alexey V. Streletskii,[§] Thomas Drewello,[§] Simona Barison,[||] Alessandro Venturini,[⊥] Francesco Zerbetto,[†] and Francesco Paolucci*[,†]

INSTM, Section of Bologna, Dipartimento di Chimica "G. Ciamician", Alma Mater Studiorum, Università di Bologna Via Selmi 2, 40126 Bologna, Italy, Sincrotrone Trieste S.C.p.A., s.s. 14 km 163.5 in Area Science Park, 34012-Trieste, Italy, Department of Chemistry, University of Warwick, Coventry CV4 7AL, England, IENI-CNR, Corso Stati Uniti 4, 35127 Padova, Italy, and ISOF-CNR Via P. Gobetti 101, 40129, Bologna, Italy

Received May 21, 2007; E-mail: Massimo.Marcaccio@unibo.it; Francesco.Paolucci@unibo.it

Abstract: The formidable electron-acceptor properties of C_{60} contrast with its difficult oxidations. Only recently it has become possible to achieve reversibility of more than one electrochemical anodic process versus the six reversible cathodic reductions. Here we exploit the reactivity of electrochemical oxidations of pure C_{60} to grow a film of high thermal and mechanical stability on the anode. The new material differs remarkably from its precursor since it conducts both electrons and holes. Its growth and properties are consistently characterized by a host of techniques that include atomic force microscopy (AFM), Raman and infrared spectroscopies, X-ray-photoelectron spectroscopy (XPS), secondary-ion mass spectrometry (SIMS), scanning electron microscopy and energy-dispersive X-ray analysis (SEM-EDX), matrix-assisted laser desorption/ionization (MALDI), and a variety of electrochemical measurements.

Introduction

Much of the chemistry and applications of C_{60} are based on its electron-accepting capacity. Six electrons are readily accommodated in the 3-fold degenerate lowest unoccupied molecular orbital (LUMO), while six more can be introduced in the equally 3-fold degenerate LUMO+1.[1,2] So much so that $Li_{12}C_{60}$ is stable and has long been described.[3] The dynamics of reduction of C_{60} and its derivatives has also been thoroughly characterized in solution by electrochemical means.[4] Furthermore, the electrochemical reduction of C_{60}[5] and $C_{60}O$[6] was used to achieve formation of C_{60}-based polymers. In the former case, formation of a rather intractable material made by an insoluble polymeric phase of intact functionalized C_{60} interspersed with counterions was observed, and in the case of electroreduction of fullerene epoxide, the resulting films strongly adhere to the electrode surface.[6] Furthermore, production of $(C_{60}O)_n$ films was also achieved by reduction of C_{60} in the presence of limited amounts of O_2 or $C_{60}O$ in a toluene/acetonitrile mixture.[7] Recently, the electrochemical reduction of ordered C_{60} fullerene films in aqueous solution[8] or ionic liquids[9] was reported to yield $(C_{60})_n$ polymers and hydrogenated fullerenes, $C_{60}H_m$. The polymers grow in this case three dimensionally and can be retransformed into pristine C_{60} by moderate annealing in vacuum. Solid films deposited onto the electrode surface by the simultaneous electrochemical reduction of C_{60} and a suitable transition-metal (e.g., Pd(II), Pt(II)) complex have also been described.[10]

Several different methods have been established to transform molecular C_{60} into all-carbon homopolymers: polymerization can be induced with an electron beam,[11] photons,[12] plasma discharge,[13] or application of high hydrostatic pressure and high temperatures.[14] The properties of C_{60}-based polymers[15a] and electrochemically formed[15b] C_{60}-based polymers have very recently been extensively reviewed.

[†] Università di Bologna Via Selmi 2.
[‡] Sincrotrone Trieste S.C.p.A.
[§] University of Warwick.
[||] IENI-CNR.
[⊥] ISOF-CNR.

(1) Haymet, A. D. J. *Chem. Phys. Lett.* **1985**, *122*, 421.
(2) Disch, R. L.; Schulman, J. M. *Chem. Phys. Lett.* **1986**, *125*, 465.
(3) Bausch, J. W.; Prakash, G. K. S.; Olah, G. A.; Tse, D. S.; Lorents, D. C.; Bae, Y. K.; Malhotra, R. *J. Am. Chem. Soc.* **1991**, *113*, 3205.
(4) Fox, M. A.; Colapret, K. A.; Hurst, J. R.; Soulen, R. L.; Maldonado, R.; Echegoyen, L. *J. Org. Chem.* **1992**, *57*, 3728.
(5) Strasser, P.; Ata, M. *J. Phys. Chem. B* **1998**, *102*, 4131.
(6) (a) Fedurco, M.; Costa, D. A.; Balch, A. L.; Fawcett, W. R. *Angew. Chem., Int. Ed. Engl.* **1995**, *34*, 194. (b) Winkler, K.; Costa, D. A.; Balch, A. L.; Fawcett, W. R. *J. Phys. Chem.* **1995**, *99*, 17431.
(7) (a) Winkler, K.; Costa, D. A.; Fawcett, W. R.; Balch, A. L. *Adv. Mater.* **1997**, *9*, 153. (b) Krinichnaya, E. P.; Moravsky, A. P.; Efimov, O.; Sobczak, J. W.; Winkler, K.; Kutner, W.; Balch, A. L. *J. Mater. Chem.* **2005**, *15*, 1468.
(8) Janda, P.; Krieg, T.; Dunsch, L. *Adv. Mater.* **1998**, *10*, 1434.
(9) Deutsch, D.; Tarábek, J.; Krause, M.; Janda, P.; Dunsch, L. *Carbon* **2004**, *42*, 1137.
(10) (a) Nagashima, H.; Nakaoka, A.; Saito, Y.; Kato, M.; Kawanishi, T.; Itoh, K. *J. Chem. Soc., Chem. Commun.* **1992**, 377. (b) Balch, A. L.; Costa, D. A.; Winkler, K. *J. Am. Chem. Soc.* **1998**, *120*, 9614. (c) Winkler, K.; de Bettencourt-Dias, A.; Balch, A. L. *Chem. Mater.* **1999**, *11*, 2265. (d) Winkler, K.; de Bettencourt-Dias, A.; Balch, A. L. *Chem. Mater.* **2000**, *12*, 1386. (e) Winkler, K.; Balch, A. L. *C. R. Chim.* **2006**, *9*, 928. (f) Plonska, M. A.; de Bettencourt-Dias, A.; Balch, A. L.; Winkler, K. *Chem. Mater.* **2003**, *15*, 4122. (g) Hayashi, A.; Yamamoto, S.; Suzuki, K.; Matsuoka, T. *J. Mater. Chem.* **2004**, *14*, 2633. (h) Grodzka, E.; Nieciecka, M.; Winkler, K. *J. Solid State Electrochem.* **2007**, DOI 10.1007/s10008-007-0358-5.

 10.1021/ja0733179 CCC: $40.75

The present paper describes the serendipitous discovery that, when operating in the presence of very low levels of nucleophiles, C_{60} may be oxidatively electropolymerized, thus forming stable conducting polymeric films able to transport both holes and electrons, a feature that is not possessed by many organic systems. The chemistry of oxidized C_{60} is less advanced, despite the fact that many organic materials base their suitability for applications, for instance, in organic electronics, on their ability to generate and transport holes. This drawback of C_{60} was recently tamed. While the first observation of electrochemically reversible one-electron oxidation of C_{60} at $E_{1/2} = 1.26$ V (vs Fc^+/Fc) was achieved by Echegoyen et al. in 1993,[16a] more recently the preparation of stable solutions of C_{60}^+ was reported[16b] and the electrochemical oxidation processes above the first oxidation were made reversible.[16c] This was a nontrivial feat since fullerenium cations react very rapidly with any nucleophile present in solution, thus giving irreversibility.

Experimental Section

Reagents. All materials were reagent-grade chemicals. C_{60} was purchased from Bucky USA (99.5%). Solvent dichloromethane (DCM) from Fluka was refluxed over and successively distilled from B_2O_3 and activated 4 Å molecular sieves. It was stored in specially designed Schlenk flasks over 3 Å activated molecular sieves, protected from light, and kept under vacuum prior to use. For the electrochemical experiments, the solvent was distilled into the electrochemical cell, prior to use, using a trap-to-trap procedure. Such a procedure avoids any contamination of the experimental environment by traces of water and oxygen as shown by the absence of any voltammetric peak associated to such species in the baseline curve (see Figure S1A).[17] The supporting electrolyte tetrabutylammonium hexafluoroarseniate ($TBAAsF_6$) was synthesized by metathesis reactions from tetrabutylammonium bromide with lithium hexafluoroarseniate (from Aldrich) and twice re-crystallized following the procedures reported in the literature.[18] Carborane $[CH_3(C_4H_9)_3]NCB_{11}H_6Cl_6$ ($MTBACB_{11}H_6Cl_6$) was a gift from Prof. C. A. Reed, University of California, Riverside, and used as received.

Cyclic Voltammetry and Spectroelectrochemistry. The one-compartment electrochemical cell was of airtight design with high-vacuum glass stopcocks fitted with either Teflon or Viton O rings in order to prevent contamination by grease. The connections to the high-vacuum line and the Schlenk flask containing the solvent were obtained by spherical joints also fitted with Viton O rings. The pressure measured in the electrochemical cell prior to performing the trap-to-trap distillation of the solvent was typically $1.0-2.0 \times 10^{-5}$ mbar. The working electrode was a Pt disc (diameter, 125 or 25 μm) or wire (area, 0.125 cm^2) sealed in glass. The counterelectrode consisted of a platinum spiral, and the quasi-reference electrode was a silver spiral. The quasi-reference electrode drift was negligible for the time required by a single experiment. Both the counterelectrode and reference electrode were separated from the working electrode by ~0.5 cm. Potentials were measured with respect to the ferrocene standard. $E_{1/2}$ values correspond to $(E_{pc} + E_{pa})/2$ from CV. Ferrocene was also used as an internal standard for checking the electrochemical reversibility of a redox couple.

Voltammograms were recorded with a AMEL model 552 potentiostat or a custom-made fast potentiostat[19] controlled by an AMEL model 568 function generator. The optical and electrochromic properties of the films were investigated by replacing the platinum support with an indium-doped tin oxide (ITO) optically transparent electrode for the electrochemical growth of the film. The growth curves obtained at the electrode were very similar to those obtained on platinum, and films having similar average thickness were prepared and transferred into the apparatus for the in-situ spectroelectrochemical investigation. Ultraflat ITO (sample gift from Kuramoto Seisakusho Co., Ltd., Tokyo, Japan) was similarly used as electrodes for AFM investigations. Electronic absorption spectra were obtained using a VARIAN Cary 5 UV-vis-NIR spectrophotometer. The CV curves are plotted versus the silver quasi-reference electrode unless otherwise indicated. All the films used for spectroscopic or mass spectrometric characterizations were grown, unless otherwise indicated, by potentiodynamic (CV) deposition and cycling the potential between 1.95 and either 0 or −1.80 V until a steady-state CV curve was obtained.

Atomic Force Microscopy. AFM imaging and analysis were performed in air with a Digital NanoScope IIIa Multimode (Veeco, USA) using phosphorus (n) doped Si probes (spring constant, 20−80 Nm^{-1}; resonance frequency, 200−400 kHz; nominal tip radius, <10 nm) operating in tapping mode. Samples for AFM imaging were prepared on ultraflat (R_a < 0.4 nm) ITO electrodes following the potentiodynamic procedure described in the text.

Raman. Raman spectra were recorded in back-scattering geometry using a Renishaw 1000 micro-Raman spectrometer equipped with a CCD camera and microscope lens of magnification ×50. Ar^+ at 514.5 nm laser line was used as the excitation source.

FTIR. A Nicolet Magna 560 spectrometer, coupled with a Spectra-Tech Continuum microscope, was employed for micro-FT-IR analyses. This instrument operates in the 4000−650 cm^{-1} infrared region and is equipped with a mercury cadmium telluride (MCT) detector cryogenically cooled to liquid nitrogen temperature.

XPS. Photoemission spectra were measured at room temperature in ultrahigh-vacuum (UHV) conditions (10^{-10} mbar) in a modified VG ESCALAB MKII experimental chamber. Photoelectrons were excited by means of Mg Kα photons and collected using a CLAM II- 150 mm hemispherical analyzer in normal emission geometry with an overall energy resolution of about 0.8 eV. The samples were directly inserted in UHV using a fast-entry air lock and measured as received as well as after a mild annealing (50 °C) to remove the adsorbed contaminants from air. The binding energies are referred to the analyzer Fermi level in electrical contact with the sample and calibrated by assuming the Pt $4f_{7/2}$ core level at 71.1 eV.

MALDI. The MALDI experiments were performed with a reflectron time-of-flight mass spectrometer (Kompact MALDI IV, Kratos, Manchester, U.K.) using a nitrogen laser (337 nm, 3 ns) and deflecting

(11) Rao, A. M.; Eklund, P. C.; Hodeau, J. L.; Marques, L.; Nunez-Regueiro, M. *Phys. Rev. B* **1997**, *55*, 4766.
(12) (a) Rao, A. M.; Zhou, P.; Wang, K.-A.; Hager, G. T.; Holden, J. M.; Wang, Y.; Lee, W.-T.; Bi, X.-X.; Eklund, P. C.; Cornett, D. S.; Duncan, M. A.; Amster, I. J. *Science* **1993**, *259*, 955−960. (b) Zhou, P.; Dong, Z.-H.; Rao, A. M.; Eklund, P. C. *Chem. Phys. Lett.* **1993**, *211*, 337. (c) Wang, Y.; Holden, J. M.; Dong, Z.-H.; Bi, X.-X.; Eklund, P. C. *Chem. Phys. Lett.* **1993**, *211*, 341. (d) Strout, D. L.; Murry, R. L.; Xu, C.; Eckhoff, W. C.; Odom, G. K.; Scuseria, G. E. *Chem. Phys. Lett.* **1993**, *214*, 576. (e) Pekker, S.; Janossy, A.; Mihaly, L.; Chauvet, O.; Carrard, M.; Forró, L. *Science* **1994**, *265*, 1077. (f) Sun, Y.-P.; Ma, B.; Bunker, C. E.; Liu, B. *J. Am. Chem. Soc.* **1995**, *117*, 12705. (g) Cataldo, F. *Polym. Int.* **1999**, *48*, 143.
(13) (a) Takahashi, N.; Dock, H.; Matsuzawa, N.; Ata, M. *J. Appl. Phys.* **1993**, *74*, 5790. (b) Zou, Y. J.; Zhang, X. W.; Li, Y. L.; Wang, B.; Yan, H.; Cui, J. Z.; Liu, L. M.; Da, D. A. *J. Mater. Sci.* **2002**, *37*, 1043.
(14) (a) Iwasa, Y. et al. *Science* **1994**, *264*, 1570. (b) Kuzmany, H.; Winter, J.; Burger, B. *Synth. Met.* **1997**, *85*, 1173. Sundqvist, B. *Physica B* **1999**, *265*, 208. Moret, R.; Wågberg, T.; Sundqvist, B. *Carbon* **2005**, *43*, 709. Sundqvist, B.; Edlund, U.; Jacobsson, P.; Johnels, D.; Jun, J.; Launois, P.; Moret, R.; Persson, P.-A.; Soldatov, A.; Wågberg, T. *Carbon* **1998**, *36*, 657. (b) Bashkin, I. O.; Izotov, A. N.; Moravsky, A. P.; Negrii, V. D.; Nikolaev, R. K.; Ossipyan, Yu. A.; Ponyatovsky, E. G.; Steinman, E. A. *Chem. Phys. Lett.* **1997**, *272*, 32. (c) Andriotis, A. N.; Menon, M.; Sheetz, R. M.; Chernozatonskii, L. *Phys. Rev. Lett.* **2003**, *90*, 026801−1.
(15) (a) Giacalone, F.; Martín, N. *Chem. Rev.* **2006**, *106*, 5136. (b) Winkler, K.; Balch, A. L.; Kutner, W. *J. Solid State Electrochem.* **2006**, *10*, 761.
(16) (a) Xie, Q.; Arias, F.; Echegoyen, L. *J. Am. Chem. Soc.* **1993**, *115*, 9818−9819. (b) Reed, C. A.; Kim, K.-C.; Bolskar, R. D.; Mueller, L. J. *Science* **2000**, *289*, 101. (c) Bruno, C.; Doubitski, I.; Marcaccio, M.; Paolucci, F.; Paolucci, D.; Zaopo, A. *J. Am. Chem. Soc.* **2003**, *125*, 15738.
(17) (a) Paolucci, F.; Marcaccio, M.; Roffia, S.; Orlandi, G.; Zerbetto, F.; Prato, M.; Maggini, M.; Scorrano, G. *J. Am. Chem. Soc.* **1995**, *117*, 6572. (b) Paolucci, F.; Carano, M.; Ceroni, P.; Mottier, L.; Roffia, S. *J. Electrochem. Soc.* **1999**, *146*, 3357. (c) Carano, M.; Da Ros, T.; Fanti, M.; Kordatos, K.; Marcaccio, M.; Paolucci, M.; Prato, M.; Roffia, S.; Zerbetto, F. *J. Am. Chem. Soc.* **2003**, *125*, 7139.
(18) Chlistunoff, J. B.; Bard, A. J. *Inorg. Chem.* **1992**, *31*, 4582.
(19) Amatore, C. A.; Jutand, A.; Pfluger, F. *J. Electroanal. Chem.* **1987**, *218*, 361.

ions outside the mass range of *m*/z 1000−3000 for higher sensitivity. The MALDI analysis was conducted directly from the original glass support on which the film was initially polymerized. A 1 μL droplet of the DCTB (*trans*-2-[3-(4-*tert*-butylphenyl)-2-methyl-2-propenylidene]malononitrile) matrix was placed onto the film as a 10^{-1} M toluene solution and dried prior to introduction into the mass spectrometer.

SIMS. Dynamic (10^{17}−10^{18} at/cm^2) secondary-ion mass spectrometry (SIMS) analyses were performed by a customized instrument.[20] A monochromatic (6 keV) O_2^+ primary-ion beam collimated to 50 μm was generated in a mass-filtered duoplasmatron ion gun (model DP50B, VG Fisons, U.K.). An EQS1000 (Hiden, U.K.) mass energy analyzer with a high-transmission 45° sector field electrostatic energy analyzer and a quadrupole mass filter were used for negative- and positive-ion detection in counting mode. Lens and energy analyzer potentials, quadrupole electronic control units, and the detection system were controlled via a Hiden HAL IV interface. The chamber pressure was typically 5×10^{-10} mbar, while the working pressure was around 3×10^{-9} mbar. Charging phenomena in insulating materials were compensated by means of a low-energy electron flux (LEG31F electron gun, VG Microtech, U.K.). Border effects were avoided with electronic gating, since only secondary ions coming from the central 50% rastered area were collected. SIMS craters depth was measured by a Tencor P-10 mechanical profiler (Tencor, USA).

SEM-EDX. Scanning electron microscopy and energy-dispersive X-ray analysis were obtained with a Philips XL 40 scanning electron microscope equipped with an EDAX PV99 energy-dispersive X-ray spectrometer.

Results and Discussion

Electrochemical Growth of a C_{60} Film. The cyclic voltammetry, CV, curve of a dichloromethane, 0.05 M $TBAAsF_6$, solution of C_{60} shows three reversible one-electron reduction peaks that are located at $E_{1/2} = -1.06$, -1.46, and -1.89 V (values vs Fc^+/Fc) and two reversible one-electron oxidation peaks at $E_{1/2} = 1.27$ and 1.71 V.[16c] As we showed previously,[16c] the CV curve obtained under the present conditions that include in the potential scan both the reduction peaks and the first oxidation one is highly reversible (Figure S1A,B): generation of neither C_{60} radical anion and higher anions nor that of C_{60} radical cation trigger any electrochemically induced reaction. As Figure 1A reveals, on the other hand, the picture may be more complicated if doubly oxidized C_{60} is generated. Figure 1A shows multiscan CV curves of a dichloromethane solution of C_{60} run between 0 and 2.20 V, i.e., corresponding to generation of C_{60}^{2+}.[16c] The curves show the appearance of new peaks in the curve and an overall progressive current increase due to formation of a redox-active deposit onto the electrode surface. The spiky cathodic peak at 1.55 V, which is only observed during the first scans (≤10, see inset of Figure 1A), is diagnostic of adsorbed species and would suggest that a very thin film of C_{60} is deposited onto the electrode surface during the first potential scans. The peak area entails a charge that increases at each scan by ~50 μC/cm^2, thus suggesting that 2−3 monolayers are deposited during each voltammetric scan. The charge exchanged by a compact single monolayer of C_{60} is in fact ~20−30 μC/cm^2.[21]

The deposited material displays its redox activity in both the positive and the negative potential regions. Figure 1B shows subsequent CV curves performed at relatively low scan rates (≤0.4 V/s) with increasing positive switching potential, also including the first two reduction peaks of C_{60}. As the scans reach 1.95 V (corresponding to the full two-electron oxidation of pristine C_{60}, Figure 1C), the CV curve attains its final pattern. Notice the presence, during the first scans, of the same spiky

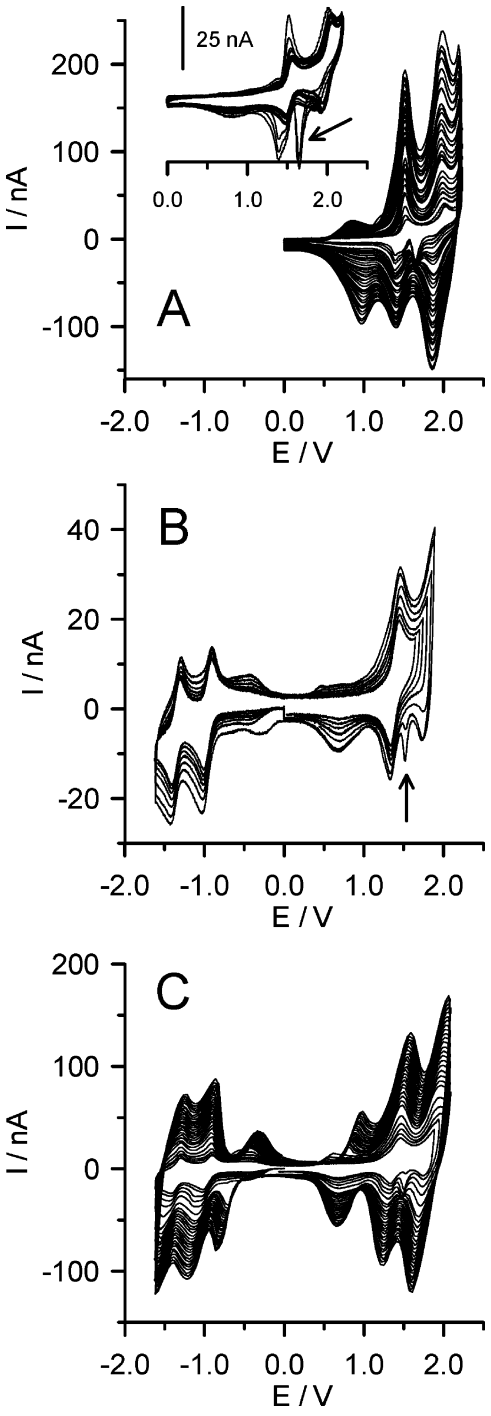

Figure 1. Cyclic voltammetric curves of a 0.15 mM solution of C_{60} in dichloromethane; the solution is 0.05 M in $TBAAsF_6$. Working electrode: Pt disk (125 μm diameter). Scan rate: 1.0 (A) and 0.4 V/s (B and C). T = 25 °C. (A) Multiscan cyclic voltammetric curves carried out between 0 and 2.2 V, showing progressive film growth. The inset displays the first (≤10) voltammetric cycles. (B) Consecutive cyclic voltammetric curves, carried out between −1.6 V and a progressively increasing positive reversal potential, suggesting film formation occurs following the second oxidation of C_{60}. (C) Following the cycles displayed in B, the multiscan cyclic voltammetric curve with constant reversal potential shows progressive film growth. In A and B, the arrow indicates the cathodic peak associated to the first few layers of adsorbed C_{60} material (see text).

(20) Tolstogouzov, A.; Daolio, S.; Pagura, C.; Greenwood, C. L. *Int. J. Mass Spectrom.* **2002**, *214*, 327.
(21) Troullier, N.; Martins, J. L. *Phys. Rev. B* **1992**, *46*, 1754.

cathodic peak at 1.55 V also observed in the growth curves obtained with positive potential scans (Figure 1A), suggesting very similar film growth dynamics in the two cases. Subsequent repetitive cycling from now on only brings about the progressive and regular increase of the current (Figure 1C), and changes in the curve pattern strongly resemble those typically observed during electrodeposition and growth of a redox-active polymeric film.[22] Importantly, while the amount of charge involved in the charging/discharging of the deposited material is almost the same in the two cases, sizable differences are observed in the curve morphology obtained with potential scans also extending to the negative potential region (Figure 1C) vis-à-vis that obtained with scans that are limited to the positive one (Figure 1A). In particular, the intense anodic peak located at ca. 1.0 V in Figure 1C is clearly coupled to the occurrence of the reduction processes occurring at $E < 0$V. Such a peak would then be associated to the discharge of entrapped (negative) charges accumulating during the film reduction(s), a behavior that is often observed in the CV of conducting and redox polymers.[22] Interestingly, an analogous cathodic prepeak (located at ~ -0.8 V) is observed in Figure 1C, evidencing that, similarly, positive charges are accumulated during the oxidation processes occurring at $E > 0$ V.

The CV curves of Figure 1 show then that the two-electron oxidation of C_{60} accumulates material on the electrode surface and that after ~10 full cycles, when the process was carried out onto an optically transparent electrode (vide infra), a smooth, red-brown film became visible to the eye. The electrochemical evolution of the film is completed after ~200 cycles when the CV current reaches the steady state. Films with the same redox and spectroscopic properties were also obtained under potentiostatic conditions, i.e., using a constant positive potential of 1.95 V, thus confirming that C_{60} anions are not involved in the film deposition and growth.

Despite of formation of a thick film onto the electrode surface, the CV curves shown in Figure 1A−C are still largely dominated by the diffusion-controlled voltammetric peaks typical of pristine C_{60} in solution. The voltammetric response of the film changes significantly in a blank electrolyte solution (Figure 2A): while the peaks due to C_{60} in solution are no longer observed, the curve still retains an overall reversible behavior that comprises two reversible redox couples at 0.8 and −0.6 V, respectively, and very broad reversible peaks located in the same potential regions where pristine C_{60} undergoes either oxidation or reduction. Therefore, the film largely retains the electroactive properties of the pristine fullerene, with significant differences that may be attributed to formation of a bonded structure where charge may be injected and transported. This is inferred from the observation that diffusion-controlled CV peaks of C_{60} in Figure 1 are only slightly affected by the presence of the film except for a large increase in intensity, in turn associated to an increase of the electroactive surface area. In particular, the separation between forward and reverse peaks has not greatly increased even in the presence of thick films (≥500 nm, vide infra), thus suggesting that the film is conductive. Attempts to measure directly the film conductivity failed because sufficiently large fragments of the film could not be detached from the conducting substrate to which it strongly adheres.

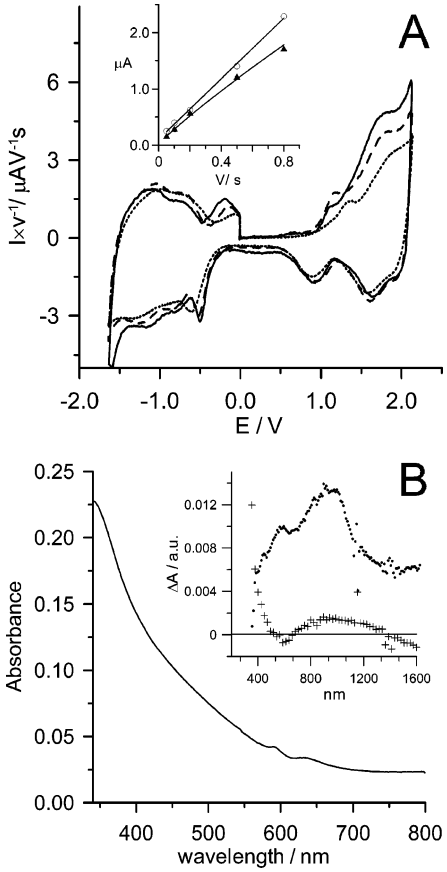

Figure 2. (A) Normalized cyclic voltammetric curves of a film-modified Pt electrode in a 0.05 M $TBAAsF_6$ dichloromethane solution. Scan rates: 0.05 (full), 0.2 (dashed), and 0.8 V/s (dotted). (Inset) Peak current intensity versus scan rate for the same system: reduction peak (empty circles) and oxidation peak (full triangles), measured at −1.2 and 1.6 V, respectively. (B) Electronic absorption spectrum of the film deposited from a 0.15 mM $TBAAsF_6$ in dichloromethane solution on a ITO electrode (see Experimental Section). (Inset) Differential absorption spectra obtained upon oxidation (crosses) at 1.4 V or reduction (dots) at −1.05 V.

Role of Electrolyte in Film Growth and Redox Dynamics. Supporting electrolytes with nucleophilic counteranions, such as ClO_4^-, BF_4^-, and, to a lesser extent, PF_6^-, are unable to sustain the regular growth of the electroactive film. The lack of growth can be ascribed to the fact that, as a rule, fullerenium radical cations react immediately in solution with nucleophiles to give C_{60} decomposition.[23]

The counteranion of choice for smooth growth is AsF_6^-. However, the CV curve obtained for a solution 0.15 mM C_{60}, 0.05 M $MTBACB_{11}H_6Cl_6$ (carborane) in dichloromethane is very similar to that obtained in the presence of $TBAAsF_6$ (Figure S1B). Indeed, carboranes form noncoordinating anions, and their very low nucleophilicity was recently exploited to prepare stable solutions of $C_{60}^{\bullet+}$ and $C_{59}N^{\bullet+}$ carbocations.[16b,23] Film growth was then obtained with the carborane-based supporting electrolyte (Figure S2A).

The availability of counterions (TBA^+ and AsF_6^-) also critically governed the dynamics of the film growth; this dependence was shown in growth experiments performed in the absence or presence of low concentrations of supporting electrolyte and at low temperature. In the absence of supporting

(22) (a) Heinze, J. In *Encyclopedia of Electrochemistry*; Bard, A. J., Stratmann, M., Schäfer, H. J., Eds.; Wiley-VCH: Weinheim, 2004; Vol. 8, p 605. (b) Deronzier, A.; Moutet, J.-C. *Coord. Chem. Rev.* **1996**, *147*, 339.

(23) (a) Reed, C. A.; Bolskar, R. D. *Chem. Rev.* **2000**, *100*, 1075. (b) Kim, K.-C.; Hauke, F.; Hirsch, A.; Boyd, P. D. W.; Carter, E.; Armstrong, R. S.; Lay, P. A.; Reed, C. A. *J. Am. Chem. Soc.* **2003**, *125*, 4024.

electrolyte, the oxidation wave is totally irreversible and there is rapid fouling of the electrode that suppresses any current in the subsequent scans (Figure S3**)**.

Analysis of the CV response of the films was carried out in a blank solution of dichloromethane and 0.05 M $TBAAsF_6$. The CV curves were obtained at various scan rates, in the 0.02−1.0 V/s range, and highly reproducible even after several (≥50) subsequent scans (Figure S4), thus indicating a remarkable stability of the redox response of the electroactive films. The above analysis showed, at low rates, that the current intensity of both reductions and oxidations scales linearly with scan rate (Figure 2A). At higher rates, $\upsilon \geq 0.4$ V/s, however, the intensity of the oxidation peak becomes proportional to the square root of scan rate. Such a behavior is often observed in the voltammetric response of conducting and redox polymers whenever diffusion of charge-compensating counterions becomes rate determining for the transport of charges.[22] The difference between oxidations and reductions in the present case would then suggest a different mobility in the film of tetraalkylammonium cations (mostly involved in the reductions) and AsF_6^- (mostly involved in the oxidations). In line with this hypothesis, carborane was found to be less efficient to promote a regular film growth and the final CV response is less reversible (Figure S2A). Interestingly, such a behavior was similar to that found with AsF_6^- when film growth was carried out at low temperature (−50 °C), where ion mobility is expectedly slower (compare Figure S2A and S2B). This suggests that film growth is less efficient with carboranes because of the much lower mobility of such bulky anions with respect to AsF_6^- within the film. Further investigation on the role of counterions in film growth and charge transport within the film using independent techniques, such as, for instance, electrochemical quartz microbalance,[7] is planned and will reported in due time.

Finally, color changes were associated to the oxidation/reduction of the redox-active film. Figure 2B shows the electronic absorption spectrum of the pristine film, while the inset displays the differential spectra obtained upon its reduction (dots) or oxidation (crosses). The absorption spectrum of the neutral film is almost featureless, as typically observed in the case of polymerized C_{60} solid films: due to formation of C−C bonds between C_{60} shells, more vibronic transition are active with respect to pristine C_{60}, thus broadening the optical absorption features. Further inhomogeneous broadening of the bands was attributed to the distribution of several oligomers usually present, for instance, in photopolymerized C_{60} films.[24] Interestingly, the differential spectrum obtained upon reduction at −1.05 V displays two main features at 950 and 590 nm, while upon oxidation at 1.40 V, a very broad and much less intense band is generated centered at ∼950 nm. Such spectral features very closely resemble those of parent fullerene radical anion and cation.[23a]

Film Morphology. The film is very stable, both chemically and mechanically, and strongly adheres to the electrode surface. SIMS and SEM measurements indicate that an average thickness ≥ 500 nm can be obtained. This thickness corresponds to >500 layers of C_{60}, assuming that neighboring monolayers may partially interpenetrate each other, and is in agreement with the observed completion of the growth after ∼200 cycles, each of which entails deposition of 2−3 monolayers. Figure 3 shows that the film uniformly coats the electrode surface.

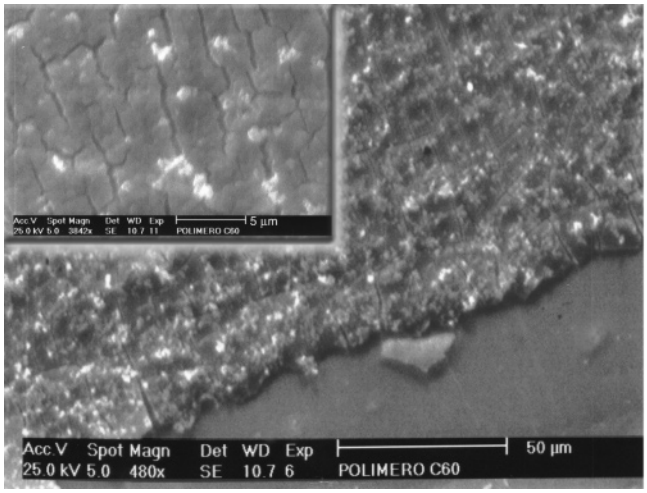

Figure 3. SEM pictures of the C_{60}-electrodeposited film on Pt (see Experimental Section).

Figure 4A−C shows the AFM images of the morphological evolution associated with an increasing number of CV cycles. From the area of the diagnostic peak at 1.55 V (see above) in the related CV growth curves, the samples correspond to approximately (A) 2, (B) 5, and (C) 20 monolayers of C_{60}.

The morphological analysis reveals that after two cycles (Figure 4A), the surface is uniformly covered with grains of materials. The surface roughness is slightly decreased with respect to the clean electrode surface, but the film does not exhibit any appreciable structure. After five cycles (Figure 4B and D), a pattern characterized by aligned nanofibers of regular dimensions, up to 50 nm in lateral size and around 0.7 nm in height (see the cross section analysis) is observed, which is compatible with the C_{60} size. Finally, after 20 CV cycles (Figure 4C), the surface has a series of undulating ridges. The growth remains directional and still yields fiber-like structures. When the nanofibers cross each other and are superimposed to those underneath, they produce the bumps observed in the AFM images. Grid-like nanostructures are distinguishable (see Figure 4E).

Nature of the Electrodeposited Film. The material electrodeposited on the electrode surface is conducting. Moreover, the electrochemical and spectroelectrochemical response of the films are strongly reminiscent of that observed in textbook examples of conducting polymers, such as polythiophene or polypyrrole[22a] or redox polymers.[22b] Quantum chemical calculations and a further physical−chemical characterization of the film was carried out to support this hypothesis.

A polymeric phase forms during the cathodic reactivity of C_{60}.[6−9] One could assume a similar behavior for the anodic processes, although, to the best of our knowledge, it is not even known if positively charged $(C_{60})_n$ is energetically stable. With the intent of ascertaining the stability of the initial steps of the polymerization to $(C_{60})_n^{n+}$, quantum chemical calculations were performed with the Gaussian03 suite of programs[25] at the B3LYP/6-31G* level.[26]

(24) Wang, Y.; Holden, J. M.; Rao, A. M.; Eklund, P. C.; Venkateswaran, U. D.; Eastwood, D.; Lidberg, R. L.; Dresselhaus, G.; Dresselhaus, M. S. *Phys. Rev. B* **1995**, *51*, 4547.

(25) Frisch, M. J. et al. *Gaussian 03*, Revision C.02; Gaussian, Inc.: Wallingford, CT, 2004.

(26) Becke, A. D. *J. Chem. Phys.* **1993**, *98*, 5648.

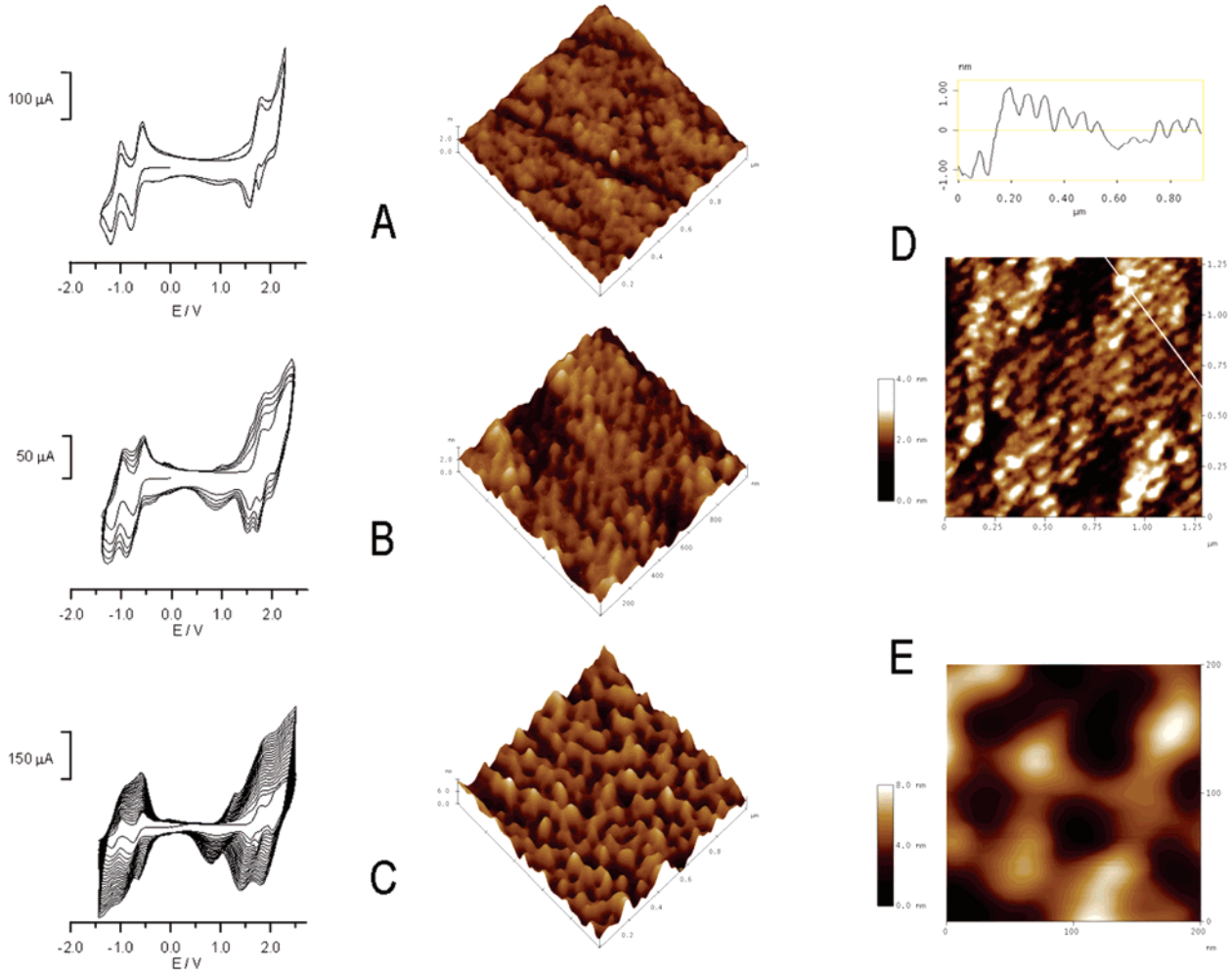

Figure 4. AFM images of the electrodeposited film of C_{60} on ultraflat ITO (see Experimental Section): (A−C) 3-D images after 2, 5, and 20 CV cycles (see the corresponding CV curves on the left). The *X* and *Y* dimensions are 1 μm (200 nm/division), while the Z scales are 4, 4, and 12 nm, respectively. (D) 2-D image after 5 CV cycles together with the cross-section analysis made along the white line. Scan size 1.25 × 1.25 μm^2. *Z* range 4 nm. (E) 2-D blow up of C, scan size 200 × 200 nm^2, *Z* range 8 nm.

The results show that the new cyclic voltammetry peaks of Figure 1 are consistent with the presence of a dimerized (or polymerized) C_{60}. The B3LYP/6-31G* HOMO energy of pristine C_{60} is 12.40 eV and reduced to 5.78 eV in the dimer. Direct comparison between the orbital energies and oxidation potentials is not possible because the former corresponds to transfer of the electron to infinite distance. However, one can use the ratio of the HOMO's energies and the corresponding ratio of the oxidation potentials for the two species. For the molecular orbitals, the ratio is 12.40/5.78 = 2.15, which compares reasonably well with that of the oxidation 1.27/0.7 = 1.8 observed experimentally.

The energies of the structures of the optimized dimers show that they are stable. These doubly charged species that can initially be formed at the anode, via the comproportionation reaction between the doubly oxidized C_{60} and pristine C_{60}, can be in the singlet or triplet state and linked by one single bond or two single bonds, see Figure 5. All four configurations were optimized and found to be minima on the potential-energy surface of $(C_{60})_2^{2+}$.

The ground state of $(C_{60})_2^{2+}$ is a triplet state with two carbon−carbon bonds of 1.598 Å that connect two hexagon−hexagon edges, one on each of the C_{60}'s, Figure 5. The singlet state of singly connected $(C_{60})_2^{2+}$ has a bond of 1.638 Å and is thermally accessible since it is only 0.5 kcal mol^{-1} higher in energy. Since this energy gap is within the accuracy of the model (of any computational model actually), it is difficult to decide if the dimerization reaction occurs via formation of a doubly linked triplet or a singly linked singlet. The energy of the doubly linked singlet is 8.3 kcal mol^{-1} higher than the ground state, while the energy of the singly linked triplet is located at 14.4 kcal mol^{-1}. Interestingly, dissociation of the singly linked singlet can take place below that of the triplet manifold with a calculated activation energy of 6.7 kcal mol^{-1}. Crossing of the two spin manifolds is expected for dissociation of doubly linked triplet $(C_{60})_2^{2+}$, which has a transition state for dissociation at 22.8 kcal mol^{-1}.

The Raman spectra of the film are dominated by two lines at ∼1570 and ∼1460 cm^{-1} (Figure 6A). The baseline shift suggests that the film is weakly photoemissive. The higher frequency line, also visible as the second dominant line in Raman studies of photoinduced, plasma-induced, pressure-induced, or electrochemically induced C_{60} polymers, is typically associated to the presence of a weakly conjugated C−C double bond.[27] The low-frequency line shows two components at 1460 and 1434 cm^{-1}, respectively. The first component is the pentagonal $A_g(2)$ pinch mode associated to the presence of linear polymeric chains in the film and usually dominant in the spectra of pressure- and

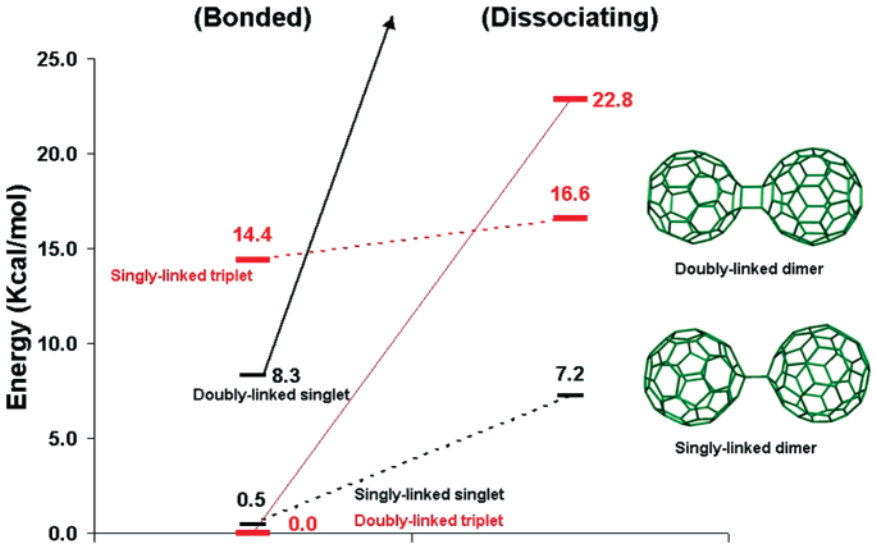

Figure 5. B3LYP/6-31G* calculations were performed to optimize the structures of the lowest singlet and triplet states of singly-linked and doubly-linked $(C_{60})_2^{2+}$.

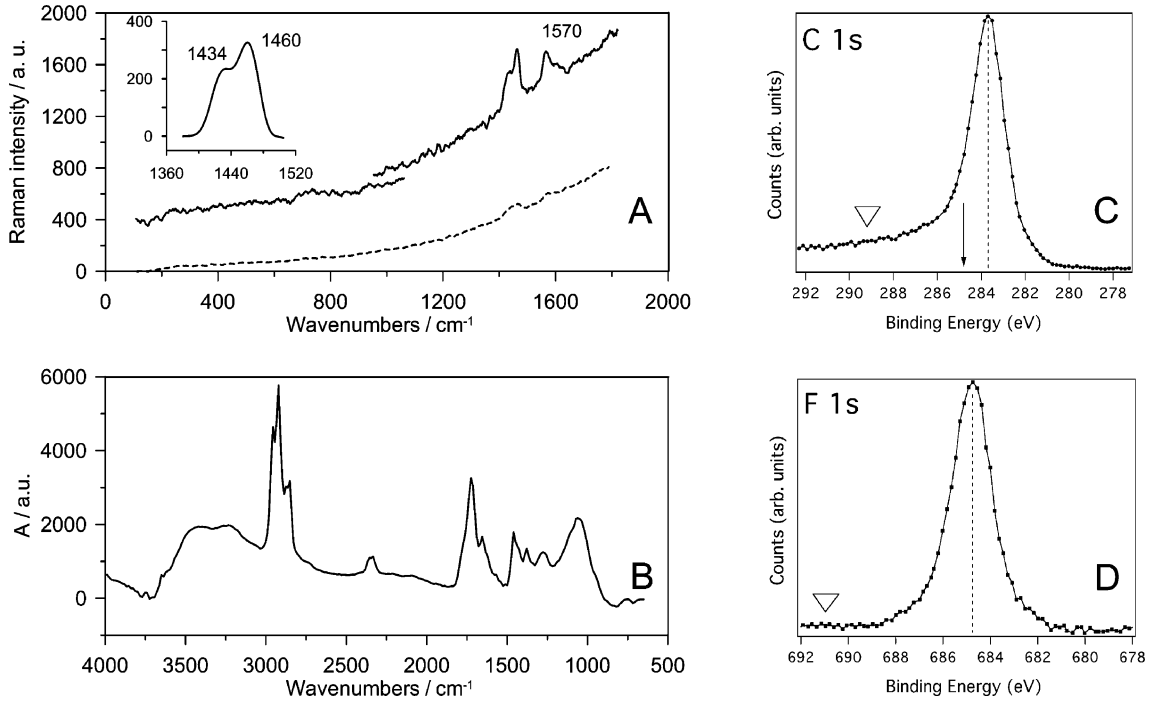

Figure 6. (A) Raman spectra of the film on platinum support. The laser excitation wavelength is 514.5 nm. (Red line) The laser power density is 200 W/cm^2, and the exposure time is 150 s. (Black line) The laser power density is 1500 W/cm^2, and the exposure time is 50 s. (B) Micro-FT-IR spectrum of the film on platinum support. (C) Photoemission spectrum of the C 1s core level. The arrow indicates the binding energy position expected in undoped non-polymeric C_{60} films. The position where the peak corresponding to carbon atoms bonded to F atoms should be expected is shown with a triangle. (D) Photoemission spectrum of the F 1s core level. The position where the peak corresponding to F atoms bonded to C atoms should be expected is shown with a triangle. For the conditions used for film deposition, see the Experimental Section.

photopolymerized films.[12a,27] The presence of this band is a particularly reliable probe of the polymerization state because the shift of this mode is very sensitive to the number of covalent bonds on the C_{60} molecules.[27] Such a component was also reported for polymers obtained by electrochemical reduction of C_{60}.[5] The lower frequency component is present, although with very small intensity, in pressure- and photopolymerized films. It is associated to two-dimensional polymers (polymeric sheets)[27a] and has not been reported so far for any electropolymerized films. The presence of this band could be therefore taken as a fingerprint of the structural peculiarity of the polymer films grown by the present electrochemical procedure. Also in agreement with the reported behavior of polymeric forms of C_{60}, the FTIR spectrum is greatly enriched with respect to pristine C_{60} (Figure 6B and Figure S5). In particular, the bands at 736, 808, 1070, 1260, 1429, and 1462 cm^{-1} have been

(27) (a) Wågberg, T.; Jacobsson, P.; Sundqvist, B. *Phys. Rev. B* **1999**, *60*, 4535. (b) Winter, J.; Kuzmany, H.; Soldatov, A.; Persson, P.-A.; Jacobsson, P.; Sundqvist, B. *Phys. Rev. B* **1996**, *54*, 17486. (c) Wågberg, T.; Persson, P.-A.; Sundqvist, B.; Jacobsson, P. *Appl. Phys. A* **1997**, *64*, 223. (d) Chambers, G.; Henderson, K.; Dalton, A. B.; Mc Carty, B.; Byrne, H. J. *Synth. Met.* **2001**, *121*, 1111.

previously attributed to active vibrational modes in fullerene polymers.[7a,12a,27d,28] Bands at 3400 and 1700 cm^{-1} indicate that water is adsorbed onto the material,[7a] and bands in the 3000−2900 cm^{-1} region are associated to the presence of tetra(*n*-butyl)ammonium ions in the film. The presence of cations from the supporting electrolyte in a film grown under oxidative conditions is not totally surprising. The film was in fact extracted from the electrolytic solution after neutralization at 0 V; however, it is known that discharging of positively charged conducting polymers involves not only the expulsion of anions but also incorporation of cations.[22] The bands in the 600−700 region (Figure S5) might in fact be associated to the As−F stretch, and the simultaneous presence of AsF_6^- anions in the film was independently confirmed by XPS and SIMS (vide infra).

The photoemission spectrum of the films deposited onto the Pt or ITO electrodes is dominated by the C 1s and F 1s peaks. The presence of a small signal due to As confirmed the hypothesis that supporting electrolyte was included in the film during the film growth (vide infra). Signals associated to the chemical elements of the supporting substrate (In, Sn, Si, and O in the case of ITO/glass) and adsorbed water were also present. Figure 6C shows the C 1s spectrum of the film deposited onto ITO/glass substrate (similar spectra were obtained for the films on Pt). Compared to pristine van der Waals molecular C_{60} films,[29,30] the C 1s is shifted by ∼1 eV to lower binding energies, indicating a more efficient screening of the core−hole consistent with formation of a conducting polymer.[31] The line width is also larger by a factor of 1.3 than that measured for pure C_{60} in similar experimental conditions.[30] This broadening can be due to a combination of an increased number of nonequivalent carbon sites, an increased phonon contribution, disorder, and a reduced core−hole lifetime in a solid-state polymer. While in C_{60} the C 1s line shape is symmetric, in the present film the line shape is asymmetric with a tail in the high binding energy side. This is typical of conducting systems or systems with a nonvanishing density of states at the Fermi level,[32] although it may equally well result from superimposition of C 1s peaks corresponding to at least four carbon atoms in a different covalent environment.[33]

Importantly, XPS measurements evidenced that there is no reaction between the counterions and C_{60}. Addition of F atoms from AsF_6^- onto the fullerene cage was in fact a possible drawback of the present anodic electropolymerization route. Fingerprints of the F−C bonds are C 1s and F 1s core level peaks around 289 and 690 eV,[34] while here the F 1s binding energy is 684.7 eV (Figure 6D). This binding energy and the atomic ratio F:As $\approx$ 6 are consistent with the presence of supporting electrolyte [(TBA)AsF_6] entrapped into the polymeric matrix. The presence of arsenic and fluorine in the film was also independently confirmed by EDX analysis of the film and SIMS analysis (Figures S6 and S9, respectively).

Matrix-assisted laser desorption/ionization (MALDI) mass spectrometry was applied to the electrodeposited film. Direct detection of undissociated oligomeric $(C_{60})_n$ ions is difficult because the intercage bond is very weak. The spectrum of the film was compared with that of pristine C_{60} studied under identical conditions (Figure S7). The region of the $(C_{60})_n^+$ species contains several peaks and reveals formation of larger clusters only for the electrodeposited film. Compared with monomeric films, photopolymerized C_{60} and C_{70} films display a markedly enhanced tendency to produce larger carbon cluster ions upon laser desorption ionization.[35] Although a variety of different processes may contribute to formation of these larger carbon clusters, their occurrence may provide a clear distinction between a pristine C_{60} target and a C_{60} film that has undergone considerable polymerization. The laser desorption-ionization time-of-flight mass spectrometry of the electrochemically prepared film (Figure S8) was observed at laser powers that were verified to avoid the photoinduced polymerization of evaporated C_{60} films. The LDITOF-MS displays the typical peak profiles of $(C_{60})_n$, for $n = 2-4$, each peak comprising several peaks separated by units of C_2. As also observed in the case of LDITOF-MS of fullerene polymers obtained by photopolymerization or plasma irradiation,[35] the maximum mass values of the polymer peaks do not coincide with multiples of C_{60} mass because of fragmentation of the fullerene polymer units during desorption.

Finally, SIMS analysis confirmed homogeneous composition all along the film thickness. The ion spectra are dominated by signals related to C_x^- clusters (Figure S9). Fluorine or boron and chlorine were detected in the case of films grown in the presence of $TBAAsF_6$ or $MTBACB_{11}H_6Cl_6$, respectively (Figure S10), confirming the homogeneous in-depth distribution of supporting electrolyte within the films.

Conclusion

Electrochemical oxidation of C_{60} to the dication triggers production of stable films onto the electrode surface that was characterized as a polymeric material. Remarkably, this approach does not require the use of functionalized C_{60}. The neutral films exposed to air and solvents showed a remarkable stability and did not undergo any significant degradation under electrochemical oxidation or reduction conditions, provided that highly aprotic and non-nucleophilic conditions were used. The film stability was particularly noteworthy since dimeric C_{120}[36] as well as linear polymers of C_{60}[37] are expected to fall apart upon reduction and was attributed to heavy cross linking between chains that typically characterize conducting polymers grown electrochemically.[22] Finally, the material transports both holes and electrons, a feature that is not possessed by many organic systems and was not previously reported for any homopolymer of C_{60}. Quantum chemical calculations suggest that sp^3 carbon centers form at the site of polymerization, thus preventing formation of a fully conjugated structure. Charge transport has

(28) (a) Yamawaki, H.; Yoshida, Y.; Kakudate, Y.; Usuba, S.; Yokoi, H.; Fujiwara, S.; Aoki, K.; Ruoff, R.; Malhotra, R.; Lorents, D. *J. Phys. Chem.* **1993**, *97*, 11161. (b) Stepanian, S. G.; Karachevtsev, V. A.; Plokhotnichenko, A. M.; Adamowitz, L.; Rao, A. M. *J. Phys. Chem. B* **2006**, *110*, 15769.
(29) Goldoni, A.; Cepek, C.; Larciprete, R.; Sangaletti, L.; Pagliara, S.; Paolucci, G.; Sancrotti, M. *Phys. Rev. Lett.* **2002**, *88*, 196102.
(30) Li, H.-N.; Wang, X.-X.; Ding, W.-F. *Surf. Sci.* **2006**, *153*, 96.
(31) Goldoni, A.; Larciprete, R.; Gregoratti, L.; Kaulich, B.; Kiskinova, M.; Zhang, Y.; Dai, H.; Sangaletti, L.; Parmigiani, F. *Appl. Phys. Lett.* **2002**, *80*, 2165.
(32) Doniach, S.; Sunijc, M. *J. Phys. C* **1970**, *3*, 285.
(33) Winkler, K.; Noworyta, K.; de Bettencourt-Dias, A.; Sobczak, J. W.; Wu, C.-T.; Chen, L.-C.; Kutner, W.; Balch, A. L. *J. Mater. Chem.* **2003**, *13*, 518.
(34) Mitsumoto, R. et al. *J. Phys. Chem. A* **1998**, *102*, 552−560. NIST XPS database, http://srdata.nist.gov/xps/.
(35) (a) Cornett, D. S.; Amster, I. J.; Duncan, M. A.; Rao, A. M.; Eklund, P. C. *J. Phys. Chem.* **1993**, *97*, 5036. (b) Ata, M.; Kurihara, K.; Takahashi, N. *J. Phys. Chem. B* **1997**, *101*, 5.
(36) Wang, G.-W.; Komatsu, K.; Murata, Y.; Shiro, M. *Nature* **1997**, *387*, 583.
(37) Sun, D.; Reed, C. A. *Chem. Commun.* **2000**, 2391.

therefore to occur within the polymeric structure principally via a hopping mechanism. Further work is planned to compare the physical−chemical properties of the material herein described with those obtained, e.g., by reductive polymerization of C_{60} and extend the novel polymerization procedure presented here to the preparation of homo- and heteropolymers of C_{60} derivatives, C_{70} and higher fullerenes.

Acknowledgment. We thank Prof. Christopher A. Reed (University of California, Riverside) for helpful discussions and a generous gift of carborane $[CH_3(C_4H_9)_3]NCB_{11}H_6Cl_6$. This research was supported by the University of Bologna and Ministero della Ricerca e dell'Università (Italy) through PRIN projects, FIRB project "Carbonio micro- e nanostrutturato", and PRRIITT project "Nanofaber". This paper is dedicated to the late Prof. Sergio Roffia (1935-2007).

Supporting Information Available: Complete refs 14a, 25, and 34; CV baseline, effects of supporting electrolyte, concentration, and temperature on the CV behavior; Material characterization (EDX, MALDI, LDITOF, and SI MS spectra); table of potential in different media. This material is available free of charge via the Internet at http://pubs.acs.org.

JA0733179